

Fig. 2. Environments of the ammonium ions viewed along the a axis. The interatomic distances between N and F atoms are given in Å. E.s.d. = 0.001 Å for all these distances. [Symmetry code: none x, y, z ; (i) $x+1, y+1, z$; (ii) $x+1, y, z$; (iii) $x+1, y-1, z$; (iv) $x, 1+y, z$; (v) $\frac{1}{2}+x, \frac{3}{2}-y, z-\frac{1}{2}$; (vi) $x, y-1, z$; (vii) $\frac{1}{2}+x, \frac{1}{2}-y, \frac{1}{2}+z$.]

In spite of satisfactory R values the standard deviations of the atomic positions are high which suggests some disorder in the structure. At room temperature strong diffuse streaks parallel to the b^* axis were observed on Weissenberg photographs. This diffuse scattering may be connected with the partial disorder in the structure and is probably related to the mechanism of the phase transition. At 334.4 K the crystal passes into the orthorhombic phase and in place of the diffuse streaks there appear quite new and sharp Bragg reflections which are consistent with the space group $P2_12_1$. The crystal structure of this phase and measurements of the lattice parameters as a

function of temperature will be the subject of a subsequent paper.

The author would like to thank Dr Z. Czaplą from the University of Wrocław for his kind provision of the crystals, Professor K. Łukasiewicz for stimulating discussions and Dr U. Rychlewska from the A. Mickiewicz University of Poznań for collecting the diffractometer data.

References

- CRUICKSHANK, D. W. J. (1956). *Acta Cryst.* **9**, 754–756, 757–758.
 CZAPLA, Z., CZUPIŃSKI, O. & WAŚKOWSKA, A. (1982). *J. Phys. Soc. Jpn.* **51**, 2693–2694.
 DEGANELLO, S. (1972). *Z. Kristallogr.* **135**, 18–33.
International Tables for X-ray Crystallography (1974). Vol. IV. Birmingham: Kynoch Press.
 ŁUKASZEWICZ, K., WAŚKOWSKA, A. & TOMASZEWSKI, P. E. (1983). *Phase Transitions*. In the press.
 MAIN, P., HULL, S. E., LESSINGER, L., GERMAIN, G., DECLERCQ, J. P. & WOOLFSON, M. M. (1978). *MULTAN. A System of Computer Programs for the Automatic Solution of Crystal Structures from X-ray Diffraction Data*. Univ. of York, England, and Louvain, Belgium.
 MAKITA, Y. & SUZUKI, S. (1980). *J. Phys. Soc. Jpn.* **48**, 693–694.
 MILKOVA, L. P. & PORAI-KOSHITS, M. A. (1962). *Izv. Akad. Nauk SSSR*, **26**, 368–377 (in Russian).
 SHELDRIK, G. M. (1978). *SHELX78*. A program for crystal structure determination. Univ. of Cambridge, England.
 STEWART, J. M. (1976). Editor, the XRAY system—version of June 1976. Computer Science Center, Univ. of Maryland, College Park, Maryland.
 WAŚKOWSKA, A., OLEJNIK, S., ŁUKASZEWICZ, K. & CIECHANOWICZ-RUTKOWSKA, M. (1979). *Ferroelectrics*, **22**, 855–861.

Acta Cryst. (1983). **C39**, 1169–1172

Structure of Orthopyroxene-Type and Clinopyroxene-Type Magnesium Germanium Oxide $MgGeO_3$

BY MITUKO OZIMA

Institute for Solid State Physics, University of Tokyo, Tokyo 106, Japan

(Received 2 February 1983; accepted 7 June 1983)

Abstract. (i) Orthopyroxene-type: $M_r = 144.92$, orthorhombic, $Pbca$, $a = 18.8099$ (12), $b = 8.9484$ (8), $c = 5.3451$ (4) Å, $V = 899.69$ (12) Å³, $Z = 16$, $D_x = 4.28$ g cm⁻³, $\lambda(\text{Ag } K\alpha) = 0.56087$ Å, $\mu(\text{Ag } K\alpha) = 75.64$ cm⁻¹, $T = 300$ K, $F(000) = 1088$, $R = 0.025$ for 975 independent reflections. (ii) Clinopyroxene-type: $M_r = 144.92$, monoclinic, $C2/c$, $a = 9.6010$ (8), $b = 8.9323$ (6), $c = 5.1592$ (5) Å, $\beta = 101.034$ (9)°, $V = 434.27$ (6) Å³, $Z = 8$, $D_x = 4.43$ g cm⁻³, $\lambda(\text{Ag } K\alpha) = 0.56087$ Å, $\mu(\text{Ag } K\alpha) = 78.35$ cm⁻¹, $T = 300$ K, $F(000) = 544$, $R = 0.021$ for 1025 independent reflec-

tions. Orthorhombic $MgGeO_3$ (the high-temperature and low-pressure phase) is isostructural with orthoenstatite, $MgSiO_3$. The structure of monoclinic $MgGeO_3$ (the low-temperature and high-pressure phase) is different from that of clinoenstatite which crystallizes in $P2_1/c$. The orthorhombic ($Pbca$) to monoclinic ($C2/c$) transformation in $MgGeO_3$ is accompanied by a fairly large volume decrease (3.5%). A smaller distortion of the Mg(2) octahedron in the structure of monoclinic $MgGeO_3$ causes the higher density.

0108-2701/83/091169-04\$01.50

© 1983 International Union of Crystallography

Introduction. Enstatite, MgSiO₃, one of the most important pyroxene-group minerals, is known to show a complicated polymorphism. Single crystals of orthoenstatite have successfully been grown by Ito (1975) and Ozima (1982) using a flux method. However, growth of single crystals of untwinned clinoenstatite has never been reported, and the structure analysis of the clinoenstatite has been carried out on the 'ortho-inverted-clinoenstatite' which contains very fine polysynthetic twinning (Morimoto, Appleman & Evans, 1960).

Germanate pyroxene, MgGeO₃, is frequently used as a convenient high-pressure model substance for the corresponding silicate, enstatite, on account of its lower transition pressure. Recently, Ozima & Akimoto (1983) have demonstrated the successful growth of single crystals of MgGeO₃ with the orthopyroxene-type structure as well as the clinopyroxene-type structure at atmospheric pressure by the flux method. They also established that the orthorhombic MgGeO₃ is the high-temperature and low-pressure phase and that monoclinic MgGeO₃ is the low-temperature and high-pressure phase. This phase relation is very similar to that of enstatite but completely different from that reported previously by Kirfel & Neuhaus (1974).

In this paper, the crystal structures of both orthorhombic and untwinned monoclinic MgGeO₃ are reported together with discussion of the transition mechanism of the orthorhombic phase to monoclinic phase in MgGeO₃.

Experimental. (i) Orthopyroxene-type: An octagonal columnar crystal formed by {210}, {100} and {010} of volume 1.0×10^{-6} cm³; Rigaku automated four-circle diffractometer, graphite-monochromated Ag K α radiation; unit-cell parameters from a least-squares fit for 30 reflections with $30^\circ \leq 2\theta \leq 45^\circ$; integrated intensities measured by 2θ - ω scans; 1197 reflections measured, 975 independent reflections ($|F_o| > 2\sigma|F_o|$) within $0^\circ < 2\theta \leq 45^\circ$, 222 unobserved, $(\sin\theta/\lambda)_{\max} = 0.682 \text{ \AA}^{-1}$, $0 \leq h \leq 25$, $0 \leq k \leq 12$, $0 \leq l \leq 7$; three standard reflections every fifty reflections; corrections for Lorentz-polarization effects and absorption (transmission factor ranged from 0.52 to 0.60); heavy atom-method, full matrix least-squares refinement on F using *RADIEL* (Coppens, Guru-Row, Leung, Stevens, Becker & Yang, 1979), unit weights, anisotropic thermal parameters for all atoms; refinements of the formal charges of the Ge and the bridging oxygen atoms were carried out; fully-ionized scattering factors for Ge⁴⁺ and Mg²⁺, orbital scattering factor for Ge, and the atomic scattering factor for O from *International Tables for X-ray Crystallography* (1974); the scattering factor for O²⁻ from Tokonami (1965); isotropic secondary extinction effect assumed [refined G factor $0.61 (2) \times 10^{-4}$]; $R = 0.025$, $wR(F) = 0.026$, $S =$

1.4474 ; final $\Delta/\sigma = 0.06$, $\Delta\rho$ in final difference map = $-0.66-0.90 \text{ e \AA}^{-3}$.

(ii) Clinopyroxene-type: A tetragonal columnar crystal formed by {110} of volume 7.8×10^{-7} cm³, confirmed to be not twinned by precession photographs in the a^*-c^* plane; unit-cell parameters obtained from a least-squares fit for 32 reflections with $30^\circ \leq 2\theta \leq 45^\circ$; 1271 reflections measured, 1025 independent reflections ($|F_o| > 2\sigma|F_o|$) within $0^\circ < 2\theta \leq 60^\circ$, 192 unobserved, $(\sin\theta/\lambda)_{\max} = 0.891 \text{ \AA}^{-1}$, $-17 \leq h \leq 17$, $0 \leq k \leq 15$, $0 \leq l \leq 9$; transmission factor ranged 0.58 to 0.67; refined G factor $7.6 (2) \times 10^{-4}$; $R = 0.021$, $wR(F) = 0.026$, $S = 1.9904$; final $\Delta/\sigma = 0.02$, $\Delta\rho$ in final difference map = $-0.44-0.72 \text{ e \AA}^{-3}$.

Discussion. Final atomic parameters are given in Table 1.† The *ORTEP* plot of the structures of the orthorhombic and monoclinic phases in MgGeO₃ is shown in Fig. 1 (Johnson, 1965). Both belong to the pyroxene structure, *i.e.* GeO₃ chains, along the c axis form the framework of the crystal. In Table 2, bond distances and bond angles are listed. It is observed that the distances between Ge and the bridging O atoms are longer than those between Ge and other O atoms. This seems to be related to a covalent character of the Ge-bridging-oxygen bond. (The valences of Ge and the bridging O atoms were found to be about +3 and -1, respectively.)

† Lists of structure factors, anisotropic thermal parameters and Table 3 have been deposited with the British Library Lending Division as Supplementary Publication No. SUP 38645 (19 pp.). Copies may be obtained through The Executive Secretary, International Union of Crystallography, 5 Abbey Square, Chester CH1 2HU, England.

Table 1. *Fractional coordinates ($\times 10^5$) and equivalent isotropic thermal parameters ($\times 10^4$) with e.s.d.'s in parentheses for orthorhombic and monoclinic MgGeO₃*

	$U_{eq} = \frac{1}{3} \sum_i U_{ii}$			
	x	y	z	$U_{eq}(\text{\AA}^2)$
(i) Orthorhombic MgGeO ₃				
Mg(1)	12336 (8)	65653 (17)	85189 (28)	80 (4)
Mg(2)	12219 (8)	48882 (18)	34352 (30)	104 (4)
Ge(1)	2780 (2)	33959 (5)	80535 (8)	69 (1)
Ge(2)	22907 (2)	34509 (5)	4141 (8)	73 (1)
O(1A)	-6455 (15)	33843 (36)	81478 (60)	89 (8)
O(2A)	6936 (17)	48881 (35)	67045 (61)	100 (9)
O(3A)	5545 (16)	31981 (35)	12519 (61)	88 (8)
O(1B)	32048 (16)	34007 (36)	2191 (56)	78 (8)
O(2B)	18768 (16)	51440 (36)	3332 (65)	104 (9)
O(3B)	19326 (16)	28958 (36)	33685 (62)	99 (9)
(ii) Monoclinic MgGeO ₃				
Mg(1)	50000	9306 (14)	75000	71 (2)
Mg(2)	50000	26954 (13)	25000	78 (2)
Ge	30016 (2)	40551 (2)	71097 (4)	54 (1)
O(1)	38248 (18)	25687 (18)	88126 (30)	79 (3)
O(2)	36065 (17)	43135 (17)	40386 (29)	71 (3)
O(3)	11635 (15)	40942 (18)	63144 (28)	67 (3)

As shown in Fig. 1 and Table 2, the orthorhombic phase of MgGeO_3 possesses two kinds of GeO_3 chains. One of the GeO_3 chains is less kinked along the c axis

Table 2 (cont.)

Table 2. *Interatomic distances* (\AA) *and interbond angles* ($^\circ$) *with e.s.d.'s in parentheses for orthorhombic and monoclinic* MgGeO_3

(i) Orthorhombic MgGeO_3	Distance	O—M—O angle
Ge(1)—O(1A)	1.739 (3)	
—O(2A)	1.708 (3)	
—O(3A ^v)	1.795 (3)	
—O(3A ^{iv})	1.799 (3)	
O(1A)—O(2A)	2.960 (4)	118.30 (14)
—O(3A ^{iv})	2.853 (4)	107.45 (14)
—O(3A ^v)	2.807 (4)	105.16 (14)
O(2A)—O(3A ^{iv})	2.787 (4)	105.20 (14)
—O(3A ^v)	2.875 (4)	110.27 (14)
O(3A ^v)—O(3A ^{iv})	2.951 (6)	110.39 (14)
Ge(2)—O(1B)	1.725 (3)	
—O(2B)	1.705 (3)	
—O(3B)	1.787 (3)	
—O(3B ^{viii})	1.762 (3)	
O(1B)—O(2B)	2.948 (4)	118.52 (14)
—O(3B)	2.962 (4)	114.99 (14)
—O(3B ^{viii})	2.840 (4)	109.08 (14)
O(2B)—O(3B)	2.586 (4)	95.55 (14)
—O(3B ^{viii})	2.919 (4)	114.69 (14)
O(3B)—O(3B ^{viii})	2.765 (6)	102.37 (14)
Mg(1)—O(1A ⁱⁱ)	2.161 (3)	
—O(1A ⁱⁱⁱ)	2.097 (3)	
—O(1B ^v)	2.055 (3)	
—O(1B ^{vii})	2.154 (3)	
—O(2A)	2.055 (3)	
—O(2B ^v)	2.004 (3)	
O(1A ⁱⁱ)—O(2A)	3.131 (4)	95.89 (13)
—O(1B ^{vii})	2.825 (4)	84.13 (12)
—O(1B ^{viii})	2.811 (4)	81.32 (12)
O(1A ⁱⁱⁱ)—O(1A ⁱⁱ)	3.107 (6)	93.72 (13)
—O(2A)	3.157 (4)	99.01 (13)
—O(1B ^{vii})	2.825 (4)	83.29 (13)
—O(2B ^v)	2.783 (4)	85.42 (13)
O(2A)—O(1B ^{vii})	2.693 (4)	81.88 (13)
—O(2B ^v)	2.961 (4)	93.66 (14)
O(1B ^{vii})—O(1B ^{viii})	3.122 (6)	95.73 (13)
—O(2B ^v)	3.031 (4)	96.60 (13)
O(1B ^{viii})—O(2B ^v)	2.919 (4)	89.11 (13)
Mg(2)—O(1A ⁱ)	2.067 (3)	
—O(1B ^{vi})	2.100 (3)	
—O(2A)	2.009 (3)	
—O(2B)	2.078 (4)	
—O(3A)	2.286 (3)	
—O(3B)	2.228 (3)	
O(1A ⁱ)—O(2A)	3.019 (4)	95.54 (14)
—O(3A)	3.078 (4)	89.85 (13)
—O(1B ^{vi})	2.811 (4)	84.85 (13)
—O(2B)	2.783 (4)	84.34 (13)
O(2A)—O(3A)	3.293 (4)	99.94 (13)
—O(1B ^{vi})	2.693 (4)	81.87 (13)
—O(3B)	3.433 (4)	108.10 (13)
O(3A)—O(2B)	3.074 (4)	89.46 (13)
—O(3B)	2.841 (4)	78.01 (12)
O(2B)—O(1B ^{vi})	2.922 (4)	88.76 (13)
—O(3B)	2.586 (4)	73.74 (13)
O(3B)—O(1B ^{vi})	3.467 (4)	106.41 (13)

Symmetry code: (i) $-x, 1-y, 1-z$; (ii) $-x, \frac{1}{2}+y, 1\frac{1}{2}-z$; (iii) $-x, 1-y, 2-z$; (iv) $x, \frac{1}{2}-y, \frac{1}{2}+z$; (v) $x, y, 1+z$; (vi) $\frac{1}{2}-x, 1-y, \frac{1}{2}+z$; (vii) $\frac{1}{2}-x, \frac{1}{2}+y, 1+z$; (viii) $x, \frac{1}{2}-y, -\frac{1}{2}+z$.

(ii) Monoclinic MgGeO_3

	Distance	O—M—O angle
Ge—O(1)	1.701 (3)	
—O(2)	1.804 (3)	
—O(3)	1.734 (2)	
—O(2 ⁱ)	1.797 (3)	
O(1)—O(2 ⁱ)	2.797 (4)	106.14 (12)
—O(2)	2.888 (4)	110.96 (13)
—O(3)	2.964 (3)	119.29 (12)
O(2)—O(2 ⁱ)	2.856 (6)	104.98 (13)
—O(3)	2.824 (4)	105.89 (12)
O(3)—O(2 ⁱ)	2.870 (4)	108.73 (12)
Mg(1)—O(1)	2.041 (3)	
—O(3 ^v)	2.069 (2)	
—O(3 ^{vi})	2.139 (3)	
O(1)—O(1 ⁱⁱⁱ)	2.845 (6)	88.39 (13)
—O(3 ^v)	3.036 (4)	95.23 (11)
—O(3 ^{vi})	3.104 (4)	95.90 (11)
—O(3 ^{vii})	2.794 (3)	85.65 (11)
O(3 ^{vii})—O(3 ^v)	2.879 (5)	86.34 (10)
—O(3 ^{vi})	2.745 (6)	79.84 (12)
O(3 ^v)—O(3 ^{vi})	3.045 (5)	92.71 (11)
Mg(2)—O(2)	2.217 (3)	
—O(3 ^v)	2.107 (3)	
—O(1 ⁱⁱⁱ)	2.021 (3)	
O(2)—O(3 ^v)	3.060 (4)	90.05 (10)
—O(1 ^{iv})	3.156 (4)	96.15 (11)
—O(1 ⁱⁱⁱ)	2.948 (4)	88.05 (11)
—O(2 ⁱⁱ)	3.363 (6)	98.63 (13)
O(3 ^{viii})—O(3 ^v)	2.745 (6)	81.30 (12)
O(1 ⁱⁱⁱ)—O(3 ^v)	2.794 (3)	85.17 (11)
O(1 ^{iv})—O(3 ^v)	2.918 (4)	89.96 (11)

Symmetry code: (i) $x, 1-y, \frac{1}{2}+z$; (ii) $1-x, y, \frac{1}{2}-z$; (iii) $1-x, y, 1\frac{1}{2}-z$; (iv) $x, y, -1+z$; (v) $\frac{1}{2}-x, \frac{1}{2}-y, 1-z$; (vi) $\frac{1}{2}-x, -\frac{1}{2}+y, 1\frac{1}{2}-z$; (vii) $\frac{1}{2}+x, -\frac{1}{2}+y, z$; (viii) $\frac{1}{2}+x, \frac{1}{2}-y, -\frac{1}{2}+z$; (ix) $\frac{1}{2}+x, \frac{1}{2}-y, \frac{1}{2}+z$; (x) $x, 1-y, -\frac{1}{2}+z$.

[O(3B^{viii})—O(3B)—O(3B^{iv}) angle = 150.25 (15) $^\circ$] than the other [O(3A)—O(3A^{iv})—O(3A^v) angle = 129.79 (14) $^\circ$]. This structure is identical with that of orthoestatite, MgSiO_3 (Morimoto & Koto, 1969). The structure of the monoclinic phase of MgGeO_3 , however, is different from that of clinostatite, MgSiO_3 (Morimoto, Appleman & Evans, 1960). Clinostatite, possesses two kinds of GeO_3 chains, similar to orthoestatite, and the space group is $P2_1/c$, while the monoclinic phase of MgGeO_3 possesses only one kind of GeO_3 chain, which corresponds to the more kinked chain in orthorhombic MgGeO_3 [O(2ⁱ)—O(2)—O(2^v) angle = 129.20 (12) $^\circ$] and the space group is $C2/c$. Thus the structure of the monoclinic phase of MgGeO_3 is similar to that of diopside ($\text{CaMgSi}_2\text{O}_6$). As indicated in Table 2, for both orthorhombic and monoclinic MgGeO_3 , the octahedral coordination of O atoms around Mg(1) is regular, while the bridging oxygen [O(3B)] of the less kinked chain [Ge(2) tetrahedron] causes the large distortion of the Mg (2)

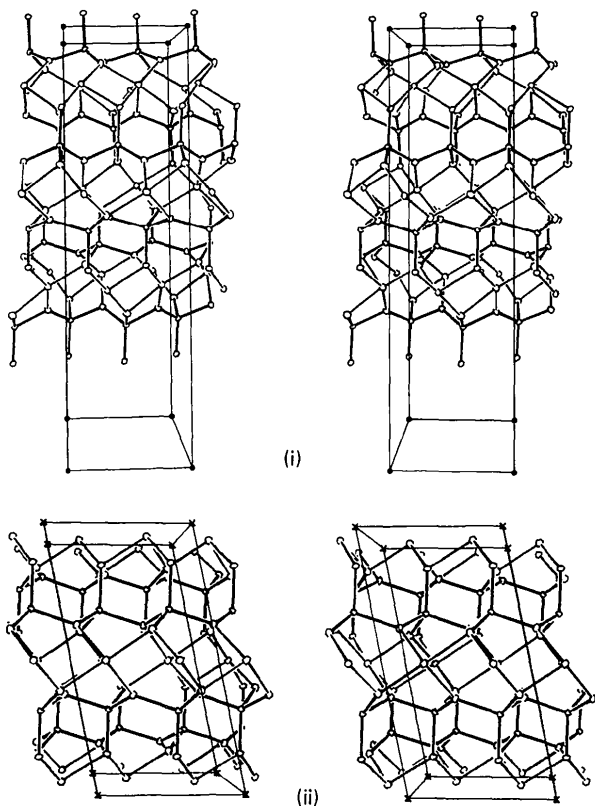


Fig. 1. Stereoscopic projection along the b axis of the structure of (i) orthorhombic and (ii) monoclinic MgGeO₃. Atoms are represented by their thermal ellipsoids with a probability of 50%.

octahedron in orthorhombic MgGeO₃. Therefore, the distortion of the Mg(2) octahedron in monoclinic MgGeO₃ is smaller than in orthorhombic MgGeO₃. One could call the structure of monoclinic MgGeO₃ 'simpler' than that of orthorhombic MgGeO₃.

In Table 3,* crystal data of silicate and germanate pyroxenes are compiled and the change in the unit-cell volume during the orthorhombic → monoclinic transformation is shown. Morimoto, Nakajima, Syono, Akimoto & Matsui (1975) have pointed out that the polymorphism relation in pyroxenes is only observed when the orthorhombic form is in space group $Pbca$ and the monoclinic in space group $P2_1/c$. No monoclinic pyroxene in space group $C2/c$ has ever been reported to have orthorhombic polymorphs ($Pbca$) except ZnSiO₃. As shown in Table 3, their observation

holds true only for silicate pyroxenes, not for germanates. ZnSiO₃ is exceptional and cannot be compared with the other pyroxenes, because Zn²⁺ in the $M(2)$ site has fourfold coordination (Morimoto, Nakajima, Syono, Akimoto & Matsui, 1975). It should be pointed out that the polymorphism between the orthopyroxene structure ($Pbca$) and the clinopyroxene structure ($C2/c$) in the germanate pyroxene induces a fairly large change in cell volume (−3.5% and −2.2% in MgGeO₃ and CoGeO₃, respectively). On the other hand, in the case of silicate pyroxene, the volume change is practically nil (+0.2 ~ −0.2%). This suggests that the pyroxene structure with $C2/c$ is more compact than that with $P2_1/c$. The large volume change could be explained by the smaller distortion of the Mg(2) octahedron in the germanate clinopyroxene in space group $C2/c$.

When Figs. 1(i) and 1(ii) are compared, the structural relations of the orthorhombic MgGeO₃ and monoclinic MgGeO₃ can be interpreted as follows. If the individual Ge(2) tetrahedron in orthorhombic MgGeO₃ rotates around the a axis, the Ge(2) chain becomes like the Ge(1) chain, increasing the shrinkage of the chain. Furthermore, if this shrunken Ge(2) chain slips about $\frac{1}{4}$ along the c axis, this structure becomes just like that of monoclinic MgGeO₃. During these operations, the Mg(2)—O(3B) bond is broken and transferred to Mg(2)—O(3B^{iv}), all other bonds being maintained. This orthorhombic—monoclinic transformation is, therefore, not martensitic.

I am very grateful to Professor S. Akimoto and Dr M. Konno of the Institute for Solid State Physics, University of Tokyo, for their help and discussions.

References

- COPPENS, P., GURU-ROW, T. N., LEUNG, P., STEVENS, E. D., BECKER, P. J. & YANG, Y. W. (1979). *Acta Cryst.* A35, 63–72.
International Tables for X-ray Crystallography (1974). Vol. IV. Birmingham: Kynoch Press.
 ITO, J. (1975). *Geophys. Res. Lett.* 2, 533–536.
 JOHNSON, C. K. (1965). *ORTEP*. Report ORNL-3794. Oak Ridge National Laboratory, Tennessee.
 KIRFEL, A. & NEUHAUS, A. (1974). *Z. Phys. Chem. Neue Folge*, 91, 121–152.
 MORIMOTO, N., APPLEMAN, D. E. & EVANS, T. H. JR (1960). *Z. Kristallogr.* 114, 120–147.
 MORIMOTO, N. & KOTO, K. (1969). *Z. Kristallogr.* 129, 65–83.
 MORIMOTO, N., NAKAJIMA, Y., SYONO, Y., AKIMOTO, S. & MATSUI, Y. (1975). *Acta Cryst.* B31, 1041–1049.
 OZIMA, M. (1982). *J. Jpn Assoc. Mineral. Petrol. Econ. Geol.* (in Japanese), Special Vol. No. 3, 97–103.
 OZIMA, M. & AKIMOTO, S. (1983). *Am. Mineral.* Submitted.
 TOKONAMI, M. (1965). *Acta Cryst.* 19, 486.

* Deposited; see deposition footnote.